J. Membrane Biol. 142, 229–240 (1994)

The Journal of
Membrane
Biology
© Springer-Verlag New York Inc. 1994

Veratridine Triggers Exocytosis in *Paramecium* Cells by Activating Somatic Ca Channels

H. Plattner, C. Braun, N. Klauke, S. Länge
Universität Konstanz, Fakultät für Biologie, Postfach 5560, D-78434 Konstanz, Germany

Received: 5 May 1994/Revised: 26 July 1994

Abstract. *Paramecium tetraurelia* wild-type (7S) cells respond to 2.5 mM veratridine by immediate trichocyst exocytosis, provided $[Ca^{2+}]_o$ (extracellular Ca^{2+} concentration) is between about 10^{-4} to 10^{-3} M as in the culture medium. Exocytosis was analyzed by light scattering, light and electron microscopy following quenched-flow/freeze-fracture analysis. Defined time-dependent stages occurred, i.e., from focal (10 nm) membrane fusion to resealing, all within 1 sec.

Veratridine triggers exocytosis also with deciliated 7S cells and with pawn mutants (without functional ciliary Ca channels). Both chelation of $Ca^{2+}{}_o$ or increasing $[Ca^{2+}]_o$ to 10^{-2} M inhibit exocytotic membrane fusion. Veratridine does not release Ca^{2+} from isolated storage compartments and it is inefficient when microinjected. Substitution of $Na^{+}{}_o$ for *N*-methylglucamine does not inhibit the trigger effect of veratridine which also cannot be mimicked by aconitine or batrachotoxin. We conclude that, in *Paramecium* cells, veratridine activates Ca channels (sensitive to high $[Ca^{2+}]_o$) in the somatic, i.e., nonciliary cell membrane and that a Ca^{2+} influx triggers exocytotic membrane fusion. The type of Ca channels involved remains to be established.

Key words: Calcium — Exocytosis — Membrane fusion — *Paramecium tetraurelia* — Veratridine

Introduction

In a variety of secretory systems Ca^{2+} plays a pivotal role in the regulation of membrane fusion during exocytosis (Cheek, 1989; Plattner, 1989; Cheek & Barry, 1993; Fasolato, Innocenti & Pozzan, 1994). This is also true for *Paramecium* cells (*see review by* Plattner et al., 1991), a ciliated protozoan. In addition to membrane fusion, Ca^{2+} is required to initiate the release of trichocyst contents by rapid decondensation (Bilinski, Plattner & Matt, 1981; Matt & Plattner, 1983). While this step clearly requires extracellular Ca^{2+} ($Ca^{2+}{}_o$), the source of Ca^{2+} for membrane fusion might be different depending on the secretagogue used. Polyamines, like aminoethyldextran (AED), induce membrane fusion (Plattner et al., 1984; Plattner, Stürzl & Matt, 1985) even in the absence of $Ca^{2+}{}_o$ (Knoll, Braun & Plattner, 1991; Knoll et al., 1993). We found, by electron spectroscopic imaging (ESI) after fast freezing, that the subplasmalemmal Ca^{2+} concentration, $[Ca^{2+}]_i$, increases during AED stimulation (Knoll et al., 1993). From both these observations, we conclude that Ca^{2+} is released from "alveolar sacs," the extensive subplasmalemmal Ca^{2+} storage compartments (Stelly et al., 1991), during AED triggering (Knoll et al., 1993). In the present work where we analyzed the other secretagogue applicable to *Paramecium,* i.e., veratridine (Knoll, Kerboeuf & Plattner, 1992), fractions of these sacs were also used in parallel to microinjection studies.

In a study on ciliary regulation, veratridine was suggested to activate *V*-dependent Ca channels (Schultz & Schade, 1989). These are the ion channels of *Paramecium* which are most extensively characterized in the literature (*see reviews by* Machemer, 1988; Preston, 1990; Preston & Saimi, 1990). While this might hold true, we show in the present paper the following aspects pertinent to exocytosis stimulation: (i) veratridine triggers exocytosis in both deciliated wild-type cells as well as in pawn mutants devoid of ciliary *V*-dependent Ca channels (for details, *see* Discussion). (ii) The stimulatory effect depends on $Ca^{2+}{}_o$, although it is inhibited by high $[Ca^{2+}]_o$.

In higher eukaryotic cells veratridine acts as a Na channel agonist, just like aconitine or batrachotoxin (for review, *see* Hille, 1992). This aspect was therefore included in our analyses, although with negative results. Another methodical aspect was the differentiation between (i) membrane fusion (dependent on $[Ca^{2+}]_i$ in-

Correspondence to: H. Plattner

crease [Lumpert, Kersken & Plattner, 1990; Plattner et al., 1991; Knoll et al., 1993]) and (ii) trichocyst decondensation (dependent on the presence of $[Ca^{2+}]_o > 10^{-5}$ M [Bilinski et al., 1981; Matt & Plattner, 1983; Knoll et al., 1991, 1993]). If (ii) were selectively inhibited, it would be difficult to ascertain aspect (i), e.g., by light microscopic (LM) analysis. Patch-clamp or electron microscope (EM) analysis would be advised. Since patch clamp analysis is not applicable to *Paramecium* cells because of their large size and rigid surface relief, we combined a new quenched-flow procedure (Knoll et al., 1991) with freeze-fracture analysis. This allowed a quantitative EM analysis of dynamic membrane events (fusion, pore expansion and resealing) in relationship to LM and light scattering analysis of exocytosis as a whole. These methods were used in parallel for mutual control and since trichocyst exocytosis has not been previously recorded by light scattering. Within the frame indicated in Results, all these evaluation methods gave well-compatible data.

Materials and Methods

Cell Cultures

Wild-type (7S) cells and the pawn mutant d4-500r (devoid of functional ciliary *V*-dependent Ca channels [Saimi & Kung, 1980; Haga et al., 1982]) were grown at 25°C to early stationary phase as described previously (Plattner et al., 1980). Under these conditions the medium contains 1.7 mM K^+, 0.4 mM Na^+ and 0.15 mM of each Ca^{2+} and Mg^{2+} (Plattner et al., 1980).

7S cells were eventually deciliated by a new protocol (M. Momayezi, this laboratory, *unpublished*), using M14 household detergent under LM control. Briefly, cells were washed in 5 mM PIPES buffer pH 7.0, supplemented with KCl and $CaCl_2$, 1 mM each. To 100 µl of cells we added 1 µl of M14 (1.0% v/v stock solution in water), immediately followed by 30 sec centrifugation (1,000 rpm in a Heraeus-Christ Minifuge [Osterode, Germany] equipped with a swing-out rotor) and addition of the same buffer, but without M14. If cells, according to LM control, were insufficiently deciliated, the time period of M14 application was extended up to 1 min. The method resulted in deciliation of ~80 to 90% of the cell surface, as observed in the LM.

Veratridine was also tested with individual deciliated cells. Veratridine was placed with a micropipette to perfectly deciliated sites (resulting in exocytosis). To exclude mechanical side-effects, controls were done by application of buffer solution only (without effect).

Chemicals and Solutions

AED was synthesized and applied as described (Plattner et al., 1984, 1985). Veratridine (Sigma, Deisenhofen, Germany) was first dissolved in HCl and titrated to pH 7.3. Other compounds listed in Results were also of the highest purity available.

Light Microscopy and Microinjections

Equal parts of cells (with cations as listed above) and of agents to be analyzed (in 10 mM Tris/HCl pH 7.3 for final use) were mixed and evaluated under a phase contrast microscope. Rating was achieved by estimating the amount of trichocysts released as described previously (Plattner et al., 1984, 1985). Since cells do not tolerate well 2.5 mM veratridine over longer time periods, samples were analyzed immediately or diluted 1:10 with buffer. Cells fully recover and can be taken in culture again when veratridine is diluted within ~20 sec after application. Deleterious effects would increasingly occur only beyond this time period.

In some experiments we microinjected 7S cells with veratridine (2.5 mM estimated final intracellular concentration) under conditions specified elsewhere (Kersken et al., 1986), using phase contrast optics. This set-up was also used for exogenous application of veratridine at sites of total deciliation, just as previously described for AED (Plattner et al., 1984).

Light Scattering Evaluation

Equal volumes of concentrated cells (250,000/ml) in culture medium and trigger (or buffer) solutions were mixed. In a control experiment trichocysts released by AED were removed by low speed centrifugation ($250 \times g \times 10$ min). Immediately after triggering samples were analyzed in a FACScan (Becton Dickinson, Heidelberg, D) cell analyzer with a 488 nm laser and 1,024 channels for measuring 90° light scattering intensities.

Quenched-Flow, Freeze-Fracture and EM Analysis

Cells were concentrated and subjected to quenched-flow analysis using AED as described by Knoll et al. (1991), or using 2.5 mM veratridine after mixing with equal volumes of cells in the apparatus (German patent 39 30 605 by H. Plattner and G. Knoll). For some experiments, cells were incubated with some other compounds to be tested, as indicated in Results.

Pt/C replicas were produced in a Balzers freeze-fracture device type BAF 300 equipped with electron beam evaporators. They were evaluated in a Zeiss EM 912 Omega or an EM 10 electron microscope. Nonoverlapping random pictures (up to six per cell) were taken at 16,000× magnification from nonselected cell membrane fractures (up to 30 evaluated per experiment). This was repeated with three independent experiments. Lower sample sizes were taken only for some pilot experiments. Evaluation of ultrastructural changes during exocytosis was carried out on 2.2× magnified prints. Stages for classification of ultrastructural changes during exocytosis were as specified previously (Olbricht, Plattner & Matt, 1984; Knoll et al., 1991).

Since freeze-fracture replicas contain small and large PF-face portions of cells, we computed the median of each of the respective stages per cell before averaging over all samples from all experiments of a specific type. This accounts for the necessarily unequal sample sizes per cell and allows for unconditional statistics. Up to 500 exocytosis sites were thus analyzed per experiment.

Experiments with Isolated Ca Stores

Subplasmalemmal Ca stores, "alveolar sacs," were isolated in purified form according to Stelly et al. (1991). Fractions contained in 20 mM Tris/maleate buffer pH 7.2 + 250 mM sucrose + 5 mM $MgCl_2$ were incubated for 30 min with 10 µM carrier-free $^{45}Ca^{2+}$ (Amersham Buchler, Braunschweig, Germany) in an adenosine-trisphosphate (ATP) regenerating system (1.5 mM ATP; 5 mM phosphocreatine + 5 U/ml phosphocreatine kinase [Sigma]), before 2.5 mM veratridine was added for additional 15 sec or 10 min in the same medium. Control and experimental samples were stopped after the same time (30 min + 15

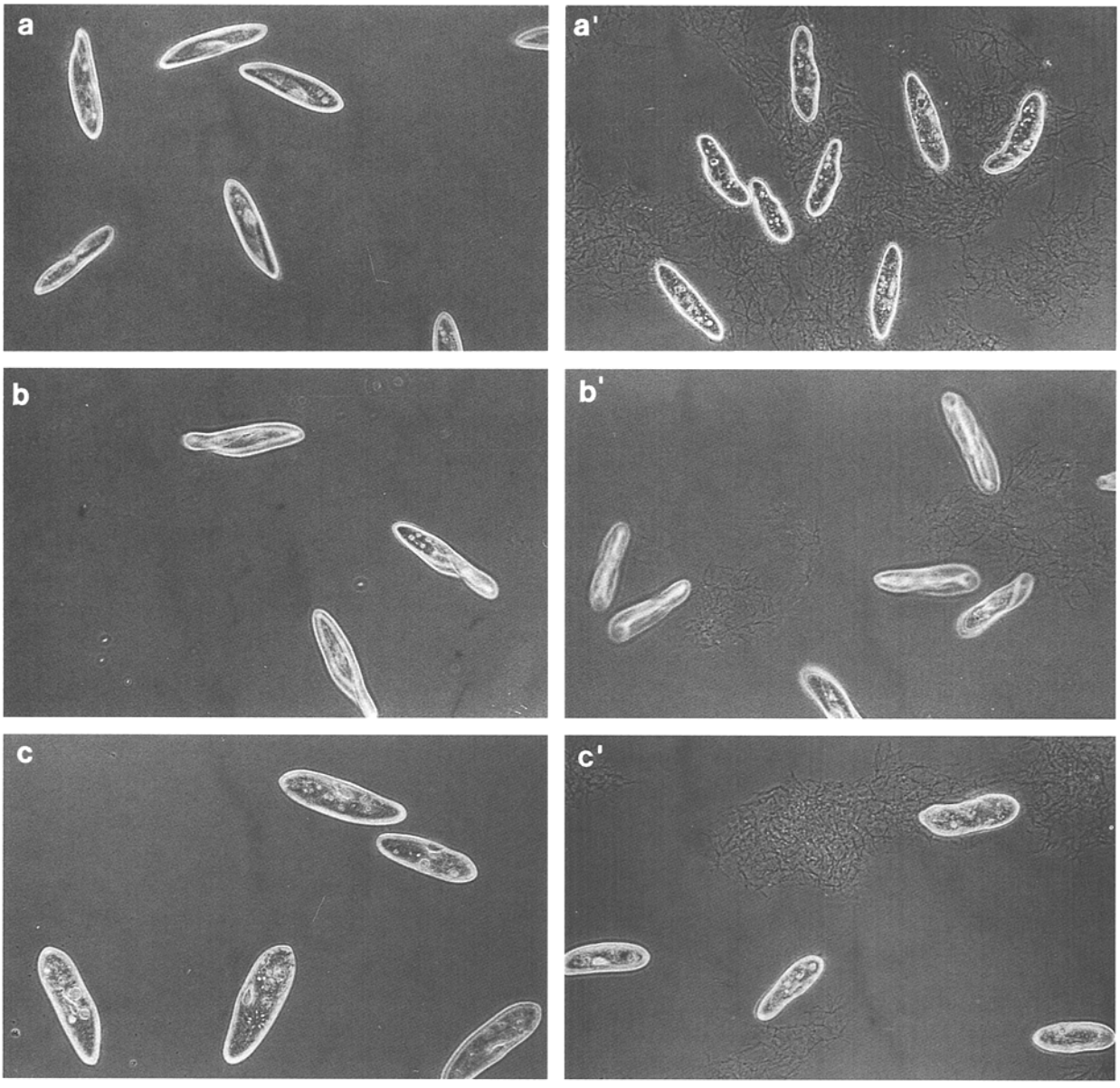

Fig. 1. LM surveys of 7S cells responding to 2.5 mM veratridine by exocytosis of needle-like, decondensed trichocysts. (*a*) Untriggered, (*a'*) after adding veratridine. (*b,b'*) Veratridine added in the presence of 10 mM Ca^{2+}, showing inhibition by Ca^{2+} (*b*) which can be overcome by adding 1.2 μM AED (*b'*). (*c,c'*) 10 mM *N*-methylglucamine has no effect per se (*c*) and does not inhibit veratridine-triggered exocytosis (*c'*). Phase contrast, 140×.

sec or 30 min + 10 min) by adding 100 μl of sample to 3 ml of ice-cold 250 mM sucrose + 40 mM NaCl pH 7.2 and washed twice in the same solution on Whatman glass microfiber filter sheaths type GF/C (Whatman Int., Maidstone, England). The radioactivity retained was measured in a Beckman liquid scintillation counter type LS 5000TD.

Results

Secretagogue Effect of Veratridine

Stimulation of trichocyst exocytosis by veratridine is documented in Fig. 1. With veratridine, higher molar concentrations are required (Knoll et al., 1992) than with the standard secretagogue, AED (Plattner et al., 1985). Table 1 summarizes EC_{50} and EC_{100} values derived from these studies. EC_{100} implies immediate release of almost all of the trichocysts docked at the cell surface, i.e., of ~95% of the whole trichocyst population, while ~5% float inaccessibly in the cytoplasm (Plattner, Knoll & Pape, 1993). In trigger experiments described below, the medium usually contained $[Ca^{2+}]_o = 0.15$ mM and $[Na^+]_o = 0.40$ mM (*see* Materials and Methods). With 2.5 mM veratridine this yields 85% exocytosis stimulation, as derived from our previous data (Knoll et al., 1992).

Table 1. EC_{50} and EC_{100} of secretagogues, AED or veratridine, applied to 7S cells[a]

Compound	EC_{50}	EC_{100}	Reference
AED, μM	1.1	1.4	Plattner et al. (1985)[c]
Veratridine, mM[b]	1.3	10.0	Knoll et al. (1992)[c]

[a] The media used for application are specified in Materials and Methods. [b]The concentration of 2.5 mM usually used releases 85% of dischargeable trichocysts. [c]For more details, *see* these references.

Figure 1 shows cells before (*a*) and immediately after adding veratridine (*a'*). Upon discharge, trichocyst contents stretch several-fold by contact with Ca^{2+} in the medium (Bilinski et al., 1981) after fusion pore formation. Therefore, the inhibitory effect of increased $[Ca^{2+}]_o$ on veratridine-triggered exocytosis (Fig. 1*b*) must be due to inhibition of membrane fusion, as ascertained in the EM (*see below*). Subsequent AED addition can overcome this inhibition (Fig. 1*b'*), since it operates over a large $[Ca^{2+}]_o$ range (Plattner et al., 1985). Since veratridine is an established Na channel agonist in higher eukaryotic systems (*see* Introduction), we ruled out this effect for exocytosis stimulation in *Paramecium,* since substituting *N*-methylglucamine for Na^+ in the medium (Fig. 1*c,c'*) or increase of $[Na^+]_o$ to 10 mM did not alter the response.

The appearance of large needles allows for quantitation by counting in the LM and by light scattering. In Fig. 2 the left scattering peak represents cells, the right one released trichocysts, for the following reasons. (i) The right-hand peak shows up only when trichocysts were released into the medium (LM control). (ii) Its height correlates with the number of trichocysts released by different concentrations of AED as an established secretagogue. (iii) It disappears when discharged trichocysts are removed. Some variation in peak position might be due to the tendency of trichocysts to aggregate. Similarly, some shift of the left peak might reflect cell contraction and/or loss of internal (condensed) trichocysts. The examples presented in Figs. 1 and 2 are representative of the rating used in Table 2, based on LM and light scattering evaluation. For example, Fig. 2 clearly reflects the trigger effect of veratridine and its inhibition by 10 mM $[Ca^{2+}]_o$. Both evaluation methods are compatible with EM analysis (*see below*) which, however, has to rely on enormously smaller sample sizes. Therefore, the different evaluation methods have been combined.

The trigger effect achieved under different experimental conditions is summarized in Table 2. It shows, in addition, that Ba^{2+} (10 mM) also inhibits veratridine stimulation, and, that as with Ca^{2+}, this inhibition can be overcome by AED. Amiloride was also tested, for reasons indicated at the end of the Discussion, but it was found to exert no effect on veratridine-triggered trichocyst exocytosis. Another result is that neither aconitine (0.25 mM) nor batrachotoxin (100 μM) trigger trichocyst exocytosis.

Irrelevance of Ciliary Ca Channels

Veratridine triggers exocytosis with deciliated 7S cells (Fig. 3*b*) equally well as with the pawn mutant d4-500r (Fig. 3*a*), as summarized in Table 2. This indicates the irrelevance of ciliary *V*-dependent Ca channels.

Since deciliation was not always complete (*see* Materials and Methods), we also applied veratridine, using a micropipette under LM control to cell surface regions showing complete deciliation (Fig. 4). Normal exocytosis always occurred at such sites. Mechanical effects were excluded by application of buffer only.

Veratridine Acts on the Cell Surface

Veratridine was also microinjected. This did not result in trichocyst exocytosis in contrast to exogenous application which also is paralleled by a $[Ca^{2+}]_i$ increase visualized by fluorochromes (*data not shown*). The final concentration of veratridine in the cell after microinjection was ~2.5 mM (as during exogenous application), as calculated from the concentration in the pipette and from the volume injected (estimated as outlined by Kersken et al., 1986). As with any injection study, local concentrations are difficult to estimate. However, injection studies with hydrophilic compounds of similar size have previously shown that the lag time between injection and recognition of the effect on the exocytotic response is short, i.e., below 1 min (Lumpert et al., 1990). This supports our assumption that veratridine exerts its trigger effect on the cell surface.

Similarly, veratridine does not release $^{45}Ca^{2+}$ from preloaded isolated Ca stores (Fig. 5), neither during short (15 sec) nor during long (10 min) time applications. These data also underscore our assumption that veratridine acts directly on the cell membrane.

Ultrastructural Analysis

EM analysis of ultrastructural changes in the cell membrane during veratridine stimulation by quenched-flow/fast freezing and freeze-fracturing is important for various reasons (*see* Introduction). Figure 6 shows typical surveys of PF-faces and Figure 7 typical details.

As described previously (*see reviews by* Plattner et al., 1991, 1993), exocytosis occurs at predetermined sites, i.e., in the middle of perpendicular ridges of the regular cell surface relief (Fig. 6*a*). An exocytosis site is delineated by a double ring of particles in whose center the site of actual membrane fusion displays a small group of large "rosette" particles in the unstimulated state

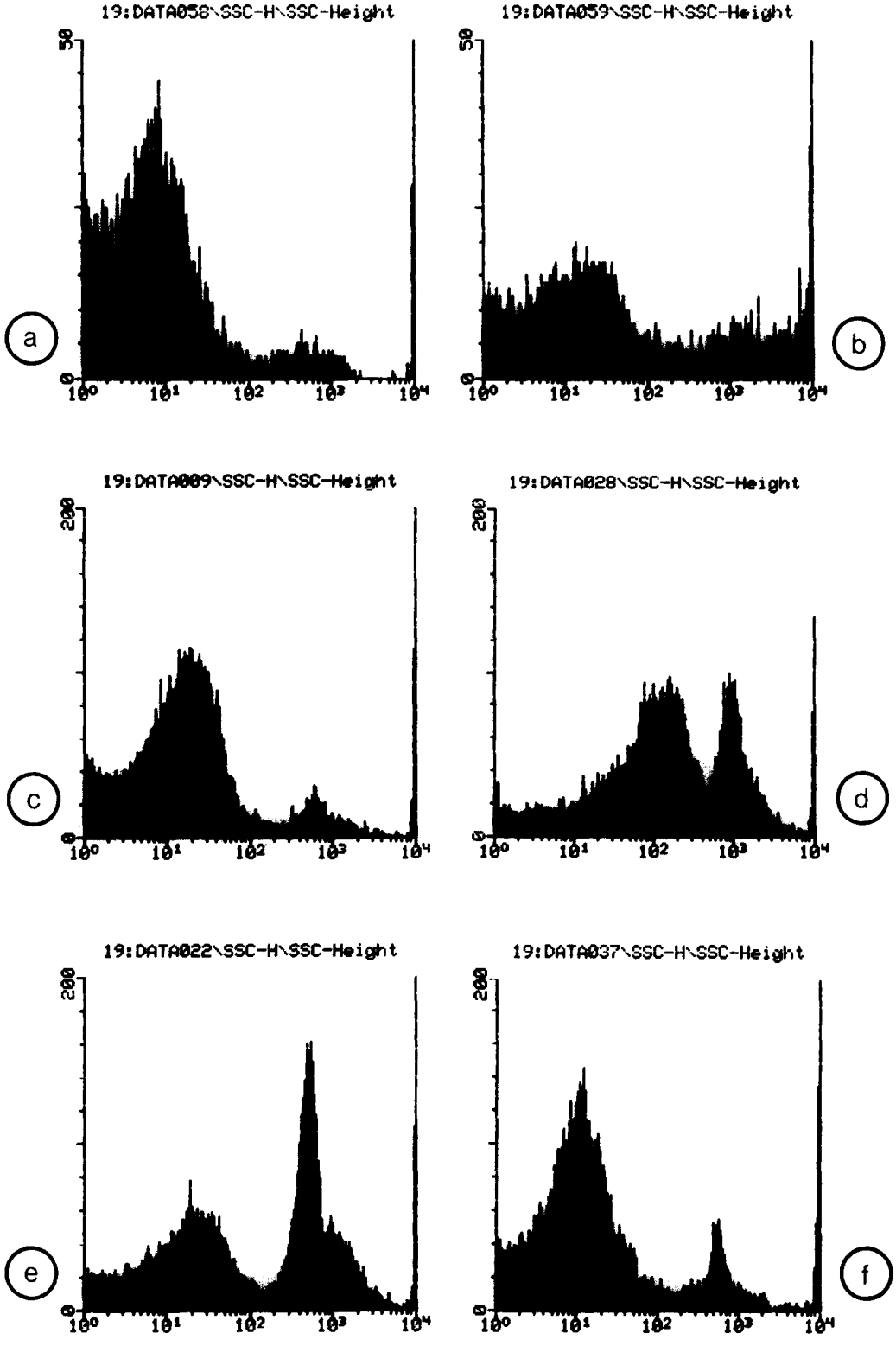

Fig. 2. Light scattering analysis of trichocyst exocytosis with 7S cells. Relative frequencies, vertical, *vs.* scattering intensity (angle), horizontal. (Data on top of diagrams are internal designations only). In addition to the peak caused by cells (left) an additional scattering peak (right) increases with increasing amounts of trichocysts released. (*a*) Untriggered cells. (*b–d*) Controls: AED-triggered cells. (*b*) Trichocysts released, but removed before assay; (*c,d*) cells triggered with EC_{10} (0.25 μM) or EC_{100} (1.25 μM) of AED and measured in the presence of released trichocysts. (*e,f*) Cells triggered with veratridine (2.5 mM) and measured in the presence of released trichocysts, (*e*) containing $[Ca^{2+}]_o$ = 0.1 mM allowing for normal exocytosis, (*f*) $[Ca^{2+}]_o$ = 10 mM which largely inhibits exocytosis.

Table 2. Exocytotic response (light microscopic evaluation)[a] to veratridine (2.5 mM) compared to other agents

Experimental set-up	Exocytotic response[a]
(A) *Wild-type cells (7S)*	
Veratridine	+++
Veratridine + Ca^{2+} (10 mM)[b]	0
Veratridine + Ca^{2+} (10 mM)[b] → AED (0.005 w/v % = 1.25 μM)	+++
Veratridine + Ba^{2+} (10 mM)[b]	0
Veratridine + Ba^{2+} (10 mM)[b] → AED (1.25 μM)	+++
Amiloride (1 mM, 1 min) → veratridine	+++
EGTA (4.5 mM) → veratridine →	0
N-methylglucamine (10 M)	0
N-methylglucamine (10 mM) → veratridine	+++
Aconitine (0.25 mM)	0
Batrachotoxin (100 μM)	0
(B) *Deciliated 7S cells*	
Veratridine	+++
(C) *Pawn cells (d4-500r)*	
Veratridine	+++

[a] Exocytotic response: rating based on quantitation by trichocyst counting and light scattering (*see* Materials and Methods). Ratings: 0, no exocytosis; +, ≤33% exocytosis; ++, 34 to 66% exocytosis; +++, 67 to 100% exocytosis (100%, all trichocysts docked at the cell periphery are exocytosed). [b]Added as chlorides.

(Figs. 6*a*, 7*a*). Exocytotic openings are abundant already 80 msec after veratridine stimulation (Fig. 6*b*), with diameters varying from "focal" fusion (Fig. 7*b*), to medium (*c*) and maximal size (*d*) equivalent to the diameter of a "ring." Figure 7*e* represents an early, (*f*) a late resealing stage, termed "filled ring" and "parenthesis," respectively. The latter indicates a collapse after detachment of empty trichocyst membranes. The stages are fully compatible with those obtained by AED stimulation and fast freezing (Knoll et al., 1991). Figure 6*c*, for instance, contains early resealing stages, thus indicating that inhibition of veratridine stimulation by high $[Ca^{2+}]_o$ has been overruled by 80 msec AED application. This fully corresponds to LM data (Fig. 1*b'*).

Quantitative evaluation shows the following (Fig. 8). In the untriggered state (*a*) 62% of docking sites are occupied by a trichocyst, as mirrored by the occurrence of a "rosette" (Plattner et al., 1991, 1993), while exocytotic openings and "filled rings" are rare or absent. "Parentheses" (nonoccupied trichocyst docking sites) contribute here by 26%. This is the normal situation (Plattner et al., 1993), thus excluding side-effects of the quenched-flow procedure. "Parenthesis" stages fluctuate between 14 and 26% throughout the whole diagram, with no systematic increase even after massive exocytosis. This has to be expected from their slow formation from "filled rings," with $t_{1/2}$ = 3 min (Plattner et al., 1993). Within 80 msec in positive controls, AED causes all "active" sites (not occupied by a trichocyst-free "parenthesis" stage) to form exocytotic openings (*b*) and no residual "rosettes" remain. Veratridine (2.5 mM) stimulates exocytosis (*c,d*), although less efficiently than AED, since the percentage of "rosettes" continues to decrease from 80 msec to 1 sec. After 80 msec of veratridine application the percentage of remaining "rosettes" is reduced from 62 to 29%, and after 1 sec to 18%. This closely corresponds to the 15% of residual (nonreleased) trichocysts to be expected (*see above*) from the established dose-response curve (Knoll et al., 1992) for the veratridine concentration applied. When EGTA is added in concentrations of 4.5 mM (resulting in a free Ca^{2+} concentration of $<0.3 \times 10^{-7}$ M, as measured by a Ca^{2+}-selective electrode [Lumpert et al., 1990]), this clearly inhibits veratridine-triggered exocytosis (*e*), as does 10 mM Ca^{2+} (*f*) or, through less efficiently, Ba^{2+} (*h*). Both phenomena can be overcome or bypassed by subsequent AED application (*g,i*). When (*g*) and (*i*) are compared with (*b*) in Fig. 8, it looks as if increased $[Ca^{2+}]$ or $[Ba^{2+}]$ would speed up the whole process of AED-elicited exocytosis. This aspect is now confirmed by more detailed analyses (H. Plattner and C. Braun, *unpublished results*). Clearly, the effect is different than with veratridine.

One has to note that in Fig. 8 columns do not always sum up precisely to 100%, because from the stochastic data (collected from many individual freeze-fractured cells) we have calculated the medians in each case before averaging (*see* Materials and Methods). The essential features outlined above are statistically significant and the same tendencies were seen in several preparations. Small discrepancies between results obtained with veratridine by LM or light scattering on one side (Figs. 1, 2, Table 2) and EM evaluation (Fig. 8) on the other side can easily be explained, because only the last method provides time resolution in the sub-second range. Furthermore, for practical reasons we could apply only suboptimal veratridine concentrations in quenched-flow experiments (*see above*). Our data might indicate that 2.5 mM veratridine would initiate exocytosis more slowly than an EC_{100} of AED, but this aspect has not been analyzed in any more detail.

Discussion

Comparison of Secretagogues

We have shown that veratridine triggers trichocyst exocytosis in *Paramecium* cells, although less efficiently than AED. This implies that the concentrations to be used are higher and that the time course observed is

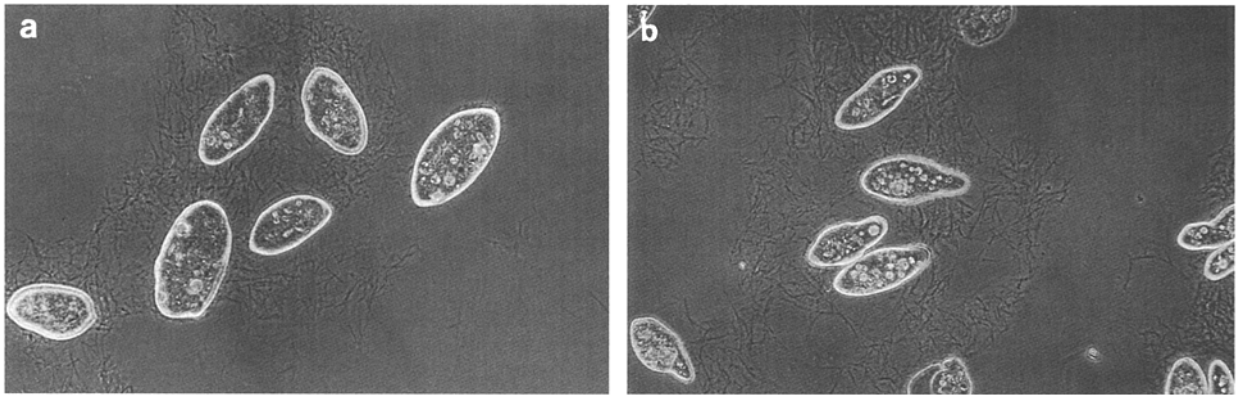

Fig. 3. Irrelevance of ciliary *V*-dependent Ca channels for the trigger effect of 2.5 mM veratridine, as shown (*a*) with the pawn mutant d4-500r and (*b*) with deciliated 7S cells. Phase contrast, 140×.

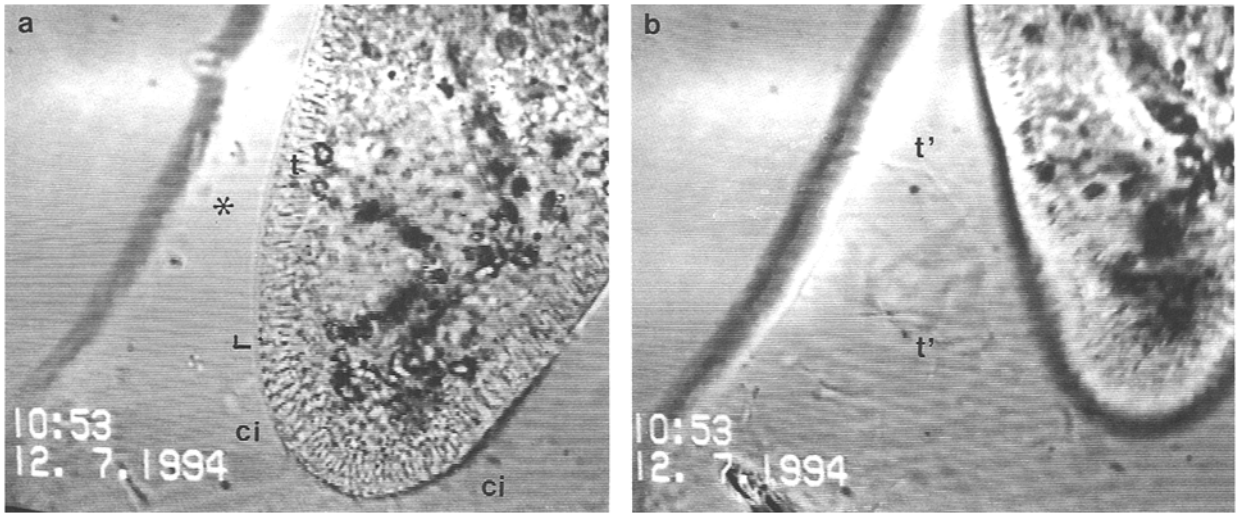

Fig. 4. Phase contrast images of a deciliated 7S cell, showing residual cilia (*ci*) at its lower end, (*a*) before and (*b*) immediately after exogenous application of 2.5 mM veratridine at the asterisk, i.e., in a region devoid of cilia (delineated by bar). Trichocysts inside the cell are labeled by *t*, those after release by *t'* (rod-like structures), respectively. Massive exocytosis from the deciliated region causes lateral displacement of the cell. 1,500×.

slower than with AED, at least under the conditions used (*see* Results). However, most importantly, veratridine causes normal ultrastructural stages of exocytosis, including focal membrane fusion, pore expansion for contents release and normal membrane resealing (Figs. 6, 7), as we could observe in previous studies with AED (Olbricht et al., 1984; Knoll et al., 1991).

In our study, toxic side-effects can be excluded as an explanation for the trigger effect of veratridine for the following reasons. (i) When veratridine is washed out after stimulation (for details, *see* Materials and Methods), cells maintain full viability and can be used for re-culturing. (ii) When veratridine stimulation is inhibited by 10 mM Ca^{2+}, cells still undergo normal (or rather accelerated) exocytosis upon subsequent AED application (Fig. 8). (iii) Ultrastructural changes accompanying veratridine-triggered exocytosis are identical as with AED which has no known side-effects (Plattner et al., 1985).

Both secretagogues can be reasonably assumed to operate via a $[Ca^{2+}]_i$ increase (*see* Introduction), since both were recently found to induce Ca-dependent currents in *Paramecium* (Erxleben & Plattner, 1994). The primary activation process must be quite different, however, since stimulation of exocytotic membrane fusion by veratridine is sensitive to $Ca^{2+}{}_o$ (Table 2), while this is not so evident with AED which operates also in the absence of $Ca^{2+}{}_o$ (Knoll et al., 1991, 1993). Although $Ca^{2+}{}_o$ is required for veratridine-stimulated exocytotic membrane fusion, too high concentrations are inhibitory, as we found. At present we cannot explain this aspect which requires more detailed analysis. The different mechanisms of veratridine and AED are also reflected by the observation that high $[Ca^{2+}]_o$, though inhibiting exo-

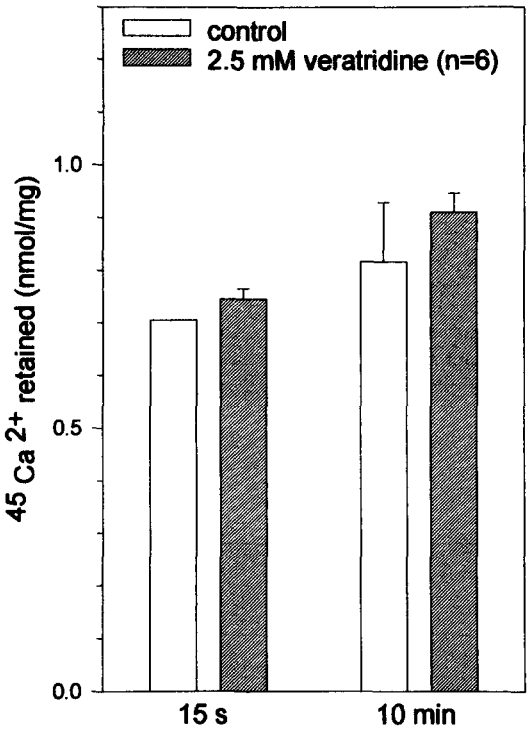

Fig. 5. Veratridine has no effect on Ca^{2+} uptake or release, as shown with isolated alveolar sacs. After 30 min preincubation with an ATP (1.5 mM) generating system in the presence of 10 μM $^{45}Ca^{2+}$, veratridine was added and the $^{45}Ca^{2+}$ retained was measured. Exposure to veratridine was for 15 sec (to check for rapid release) or 10 min (to check for slow release or latent uptake inhibition). Relative to the control after 30 min + 15 s (left), the control value after 30 + 10 min (right) has slightly increased (open bars), but no veratridine effects can be ascertained over 15 s or 10 min (shaded bars) within standard deviations.

cytosis with veratridine, allows for exocytosis with AED (Figs. 1*b,b'*, 6*c*) which it even accelerates (*see* Results). In contrast to AED, activation of intracellular Ca pools by veratridine appears less likely since it requires adequate $[Ca^{2+}]_o$ and causes neither trichocyst release after microinjection, nor Ca^{2+} release from isolated stores (*see* Results). Interestingly, such activation may occur, e.g., with some, but not all, crayfish nerve-muscle synapses (Finger & Martin, 1989). However, at present we cannot strictly exclude secondary activation of internal Ca stores, e.g., by Ca^{2+}-induced Ca^{2+} release.

On a speculative basis, our findings might imply for AED a more efficient delivery of Ca^{2+} to exocytosis sites, possibly by site-directed release from closely attached alveolar sacs (Knoll et al., 1993; Erxleben & Plattner, 1994), whereas veratridine might activate a Ca^{2+} conductance over the entire cell membrane (*see below*). In fact, exocytosis triggered by veratridine is slower than with AED (*see* Results).

Ionic Conductances Possibly Involved

Which ion channels might be involved in Ca^{2+} entry during veratridine-stimulated trichocyst exocytosis? Veratridine is a Na channel agonist in higher eukaryotic cells (Barnes & Hille, 1988; for review, *see* Hille, 1992). However, we have excluded this effect by showing that substitution of *N*-methylglucamine for Na^+ in the medium does not abolish the veratridine effect. The secretagogue effect of veratridine is independent over a wide $[Na^+]_o$ range (*data not shown*). Furthermore, other Na channel agonists, like aconitine (Mozhayeva et al., 1977; Ghiasuddin & Soderlund, 1984; Hille, 1992) or batrachotoxin (Dubois, Schneider & Khodorov, 1983; Ghiasuddin & Soderlund, 1984, Khodorov, 1985; Hille, 1992; Cordell, 1993) do not trigger exocytosis. Although this would lend further support to our arguments, it must be noted that their pharmacology in *Paramecium* has not yet been established.

In agreement with the present study, induction of a Ca conductance by veratridine was inferred by Schultz and Schade (1989). The was concluded from the induction of $Ca^{2+}{}_o$-dependent ciliary reversal by veratridine, accompanied by an increase of cGMP (guanosine 3':5'-cyclic monophosphate), on the following basis. During ciliary reversal, *V*-dependent Ca channels, which are known to be localized exclusively in ciliary membrane (Ogura & Takahashi, 1976), are activated (*see reviews by* Machemer, 1988; Preston & Saimi, 1990). Pawn mutants are defective in these channels and, thus, cannot normally perform ciliary reversal (Saimi & Kung, 1980; Haga et al., 1982). However, they do reverse their ciliary beat in response to veratridine and in parallel they produce increased levels of cGMP (Schultz & Schade, 1989), an established factor of the reversal mechanism (Schultz, Pohl & Klumpp, 1986; Preston & Saimi, 1990). Though we do not question the validity of these results for ciliary reversal, in the context of exocytosis stimulation by veratridine we have important reasons to assume stimulation of Ca conductances in the *somatic* cell membrane. (i) Pawn cells and deciliated wild-type cells release trichocysts in response to veratridine (Fig. 3). The irrelevance of ciliary Ca channels has been substantiated by local application of veratridine to individual cells in regions where they show perfect deciliation (Fig. 4). Trichocysts are released in a normal way from such sites. (ii) This is the same result previously obtained with AED (Plattner et al., 1984) which causes a similar cGMP increase (Knoll et al., 1992) as described by Schultz and Schade (1989), though AED is known *not* to activate ciliary Ca channels (Plattner et al., 1984). Thus, an increase of cGMP does *not* necessarily imply activation of cilia.

In conclusion, the secretagogue effect of veratridine must operate via the somatic part of the cell surface.

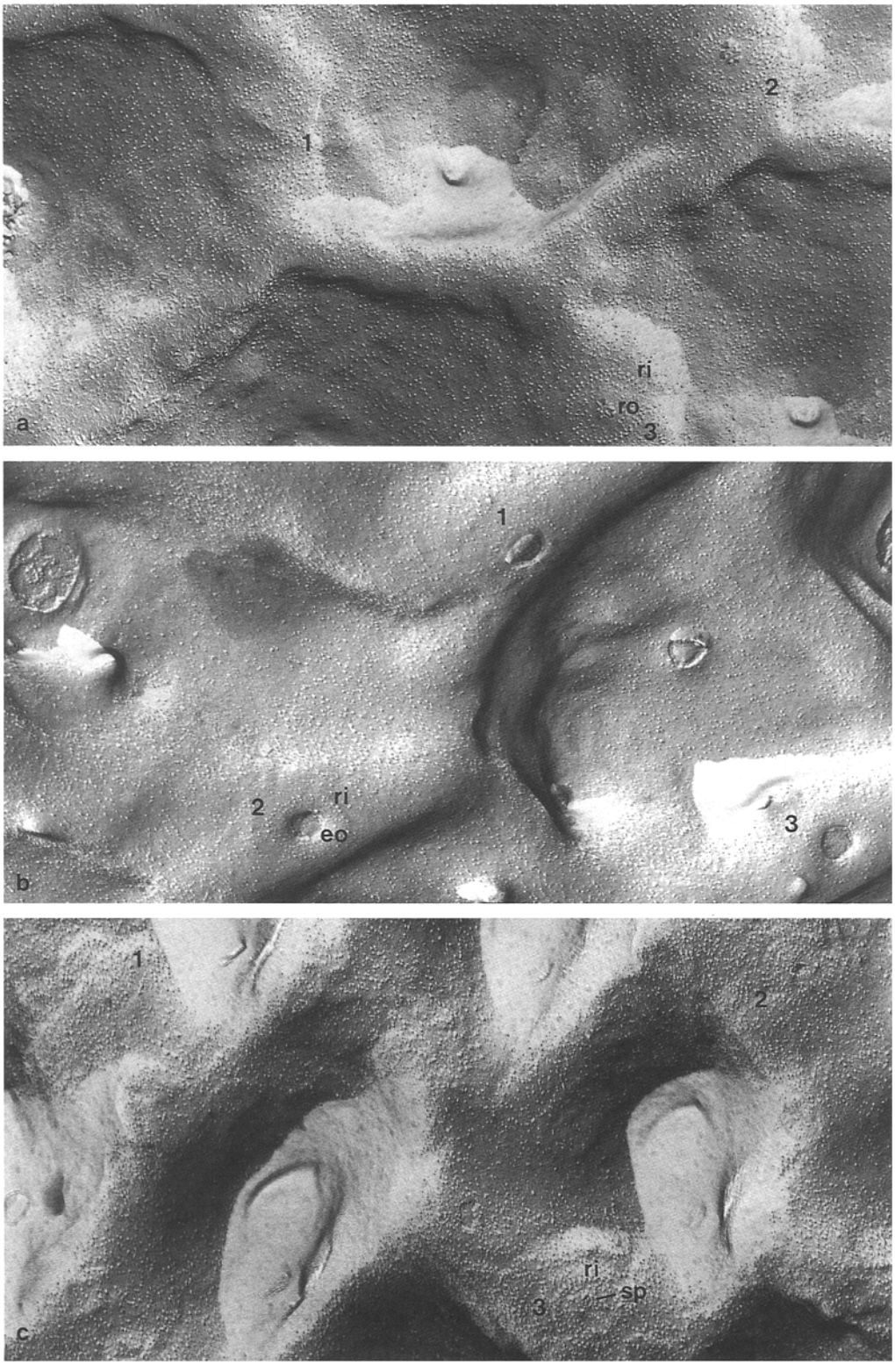

Fig. 6. Typical freeze-fracture surveys, PF-faces, of cell membranes. (*a*) Unstimulated state, (*b*) after 80 msec stimulation by 2.5 mM veratridine (quenched-flow) and (*c*) after 20 sec exposure to 2.5 mM veratridine plus 10 mM Ca^{2+} whose inhibitory effect on membrane fusion has been overcome by adding 1.2 μM AED for 80 msec in a quenched-flow analysis. At three exocytosis sites (*1–3*), within the ~300 nm large double rings (*ri*) of membrane particles delineating the exocytotically active zone, one can recognize: (*a*) a small group of large "rosette" (*ro*) particles, (*b*) exocytotic openings (*eo*) and (*c*) a large number of small particles (*sp*) typical for freshly resealed exocytosis sites. *See* Fig. 7 for enlarged views. 50,000×.

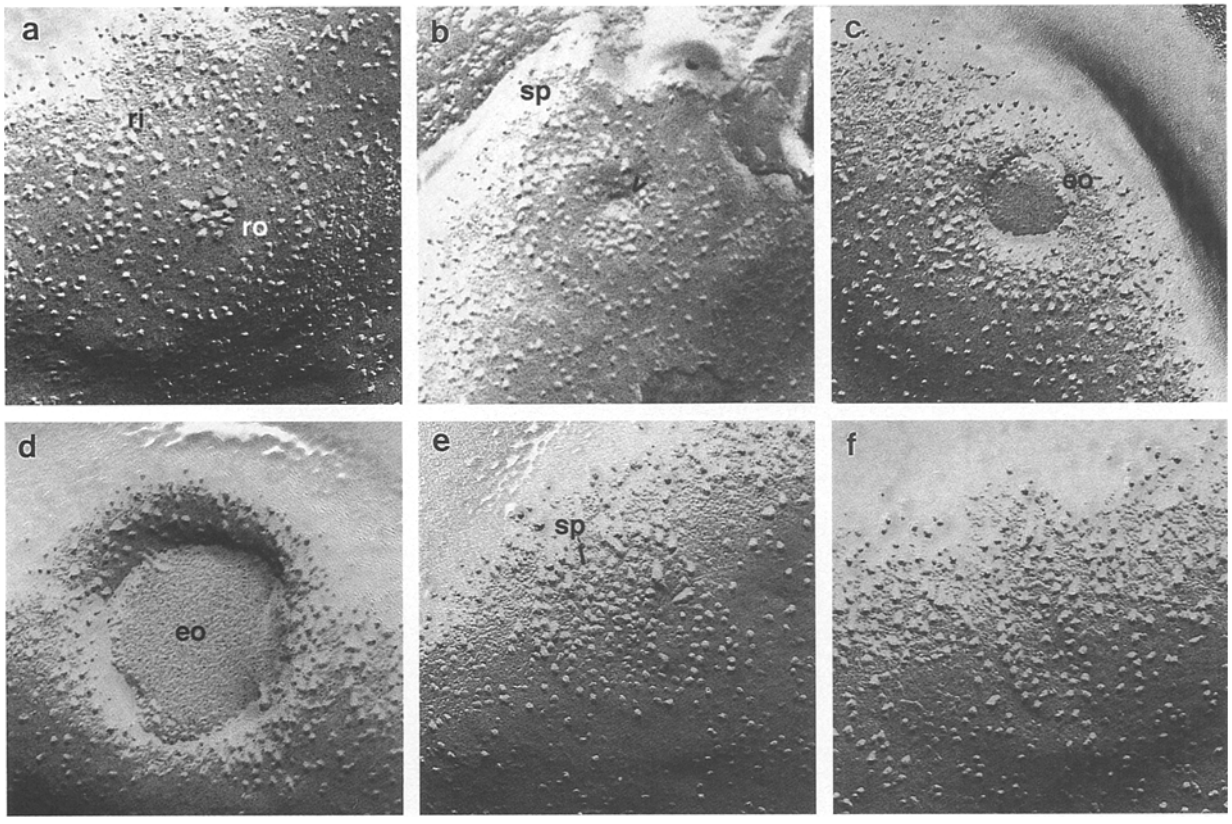

Fig. 7. Stages of membrane restructuring (fusion/opening/resealing) seen in PF-face freeze-fracture views of the cell membrane after different times of veratridine (2.5 mM) stimulation and quenched-flow analysis. Note delineation of exocytosis sites by a double particle ring (*ri*). (*a*) Unstimulated control with a small number of large rosette (*ro*) particles. (*b–d*) Increasing sizes of exocytotic pores, all observed during 80 msec veratridine stimulation. (*b*) An early focal fusion event (arrowhead) accompanied by appearance of a large number of small particles (*sp*). (*c*) An increased and (*d*) a maximally enlarged exocytotic opening (*eo*). (*e,f*) Collected 1 sec after stimulation, representing a "filled ring" with numerous small particles (*sp*) (*e*), or a "parenthesis" stage (*f*), respectively, characteristic of early or late membrane resealing stages (*see text*). Shadow casting from bottom to top. 100,000×.

Some spillover of Ca^{2+} might occur, since we frequently observe a brief ciliary reversal during AED-stimulated trichocyst release (Plattner et al., 1985), although normally regulation of exocytosis and of ciliary activity appears rather clearly separated. Just like Schultz and Schade (1989) we also observed the independence of the veratridine effect from $[Na^+]_o$ and the inhibitory effect of high extracellular Ca^{2+} or Ba^{2+} concentrations. They also noted the insensitivity to the Na channel antagonist, tetrodotoxin (TTX), which can antagonize Na^+-based veratridine effects in metazoan cells, e.g., Na^+/Ca^{2+} exchange following Na^+ entry (Kao & Cheung, 1990; Uezono et al., 1992). The inefficiency of TTX led Schultz & Schade (1989) to assume the activation of Ca channels by veratridine, as we can confirm.

The somatic cell membrane has different Ca conductances (*reviewed by* Machemer, 1988; Preston, 1990; Preston & Saimi, 1990). Which ones might contribute to veratridine stimulation? Mechanosensitive Ca channels are unlikely candidates, since they are restricted to the anterior part of the cell (Machemer, 1988; Kung, Saimi & Martinac, 1990), whereas exocytosis occurs over the whole cell surface, as shown in Results. (We also have ruled out unwanted mechanical stimulation by application of the quenched-flow precedure.) For the same reason an anterior Na channel (Saimi, 1986) can be excluded. This channel would also carry Ca, particularly in the absence of Na^+_o (Saimi, 1986), but veratridine-stimulated exocytosis does not depend on $[Na^+]_o$. A hyperpolarization-sensitive Ca channel, of so far unknown distribution over the somatic cell membrane, is defined by inhibition by 10 mM Ba^{2+} or by 1 mM amiloride (Preston, Saimi & Kung, 1992). While secretion stimulation by veratridine is inhibited by Ba^{2+}, it is not by amiloride (Table 2), and the same effect can be achieved with high $[Ca^{2+}]_o$ as with Ba^{2+}. Therefore, this Ca channel is also an unlikely candidate. How veratridine-stimulated exocytosis is related to the somatic "Ca leakage conduc-

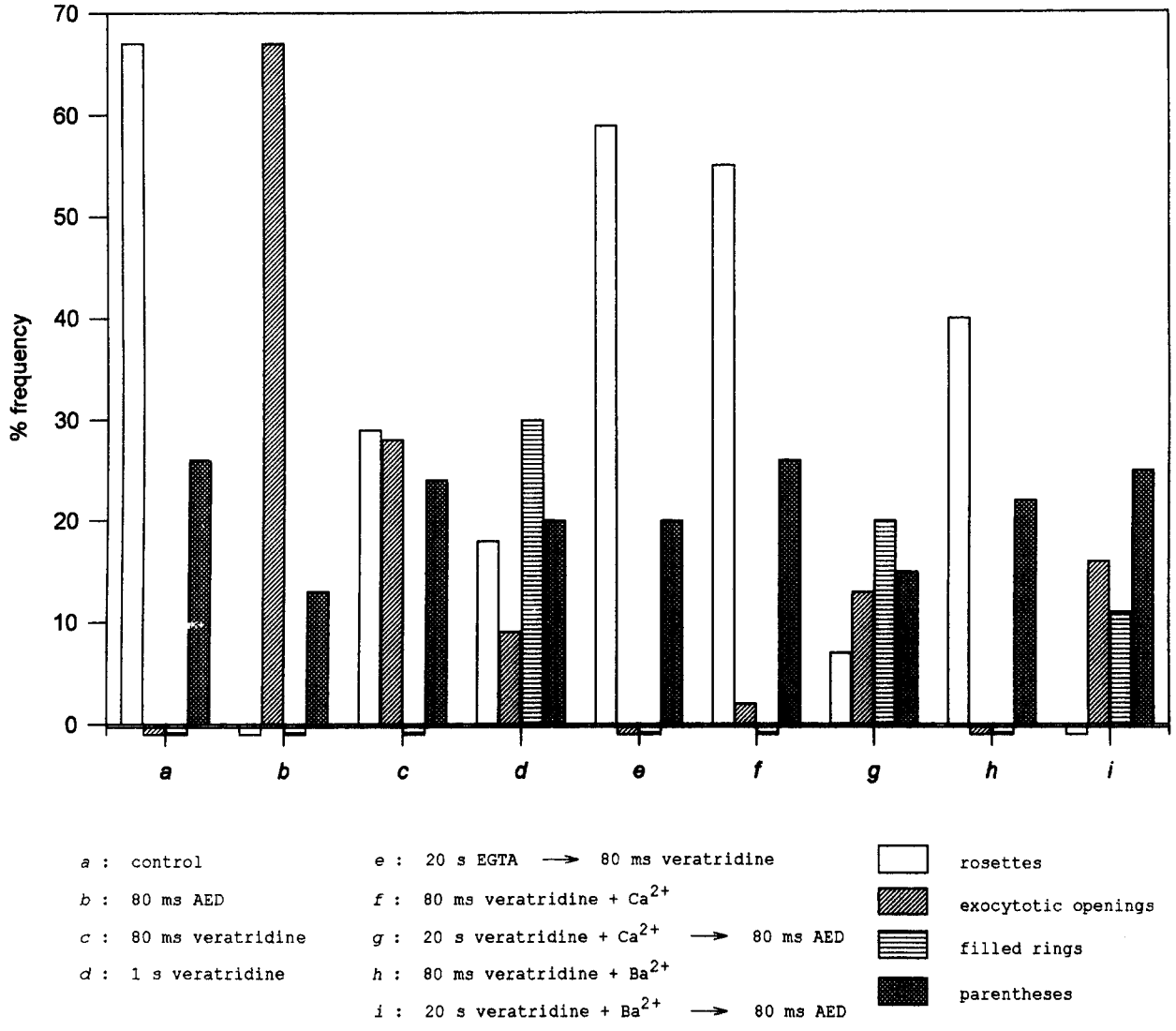

Fig. 8. Quantitative evaluation of quenched-flow/free-fracture data obtained under different conditions of exocytosis stimulation. The medium normally contained 0.15 mM Ca^{2+}. Exceptions are samples with EGTA added (4.5 mM, resulting in $<0.3 \times 10^{-7}$ M measured free $[Ca^{2+}]$ in *e*) and samples supplied with additional Ca^{2+} (10 mM in *f* and *g*). Ba^{2+} (in the presence of 0.15 mM Ca^{2+}) was also 10 mM (*h,i*). Stages are as presented in Fig. 7. Exocytotic openings of different sizes are pooled. Zero values are plotted below baseline. For more details, *see text.*

tance" (Machemer, 1988) or any other conductances remains to be settled. Interestingly, a leaky Ca conductance occurs also with pawn cells (Satow & Kung, 1980).

Conclusions

Though the nature of the Ca conductance assumed to be activated by veratridine remains unsettled, it must be localized on the somatic cell membrane. Time-resolved $^{45}Ca^{2+}$-flux measurements (as previously done with AED [Knoll et al., 1992]) as well as more extensive pharmacological and electrophysiological studies might clarify this aspect. The trigger effect of both secretagogues, AED and veratridine, appears different with regard to the origin of Ca^{2+}, although the resulting $[Ca^{2+}]_i$ increase might cause the same downstream effects. This is important for further analysis of the signal transduction pathway in stimulus-secretion coupling.

We thank Dr. C. Kung (Madison, WI) for providing the pawn mutant, Drs. G. Lehle and R. Waldschütz-Schüppel (Konstanz, Germany) for their help with light scattering experiments, and Ms. E. Dassler and D. Bliestle for continuous help during the extensive photographic documentation. This work has been supported by Deutsche Forschungsgemeinschaft, Schwerpunkt "Neue mikroskopische Techniken für Biologie und Medizin" (grant P178/11) and SFB156/B4.

References

Barnes, S., Hille B. 1988. Veratridine modifies open sodium channels. *J Gen. Physiol.* **91**:421–443

Bilinski, M., Plattner, H., Matt, H. 1981. Secretory protein decondensation as a distinct, Ca^{2+}-mediated event during the final steps of exocytosis in *Paramecium* cells. *J. Cell Biol.* **88**:179–188

Cheek, T.R. 1989. Spatial aspect of calcium signalling. *J. Cell Sci.* **93**:211–216

Cheek, T.R., Barry, V.A. 1993. Stimulus-secretion coupling in excitable cells: A central role for calcium. *J Exp. Biol.* **184**:183–196

Cordell, G.A. 1993. The Alkaloids. Chemistry and Pharmacology. Academic, San Diego, New York, Boston

Dubois, J.M., Schneider, M.F., Khodorov, B.I. 1983. Voltage dependence of intramembrane charge movement and conductance activation of batrachotoxin-modified sodium channels in frog node of Ranvier. *J. Gen. Physiol.* **81**:829–844

Erxleben, C., Plattner, H. 1994. Ca^{2+} release from subplasmalemmal stores as a primary event during exocytosis in *Paramecium* cells. *J. Cell Biol. (in press)*

Fasolato, C., Innocenti, B., Pozzan, T. 1994. Receptor-activated Ca^{2+} influx: how many mechanisms for how many channels? *Trends Pharmacol. Sci.* **15**:77–83

Finger, W., Martin, C. 1989. Quantal stores of excitatory transmitter in nerve-muscle synapses of crayfish evaluated from high-frequency asynchronous quantal release induced by veratridine or high concentrations of potassium. *Eur. J. Physiol.* **414**:337–442

Ghiasuddin, S.M., Soderlund, D.M. 1984. Mouse brain synaptosomal sodium channels: Activation by aconitine, batrachotoxin, and veratridine, and inhibition by tetrodotoxin. *Comp. Biochem. Physiol.* **77C**:267–271

Haga, N., Forte, M., Saimi, Y., Kung, C. 1982. Microinjection of cytoplasm as a test of complementation in *Paramecium. J. Cell Biol.* **92**:559–564

Hille, B. 1992. Ionic Channels of Excitable Membranes. Second edition. Sinauer, Sunderland, MA

Kao, L.S., Cheung, N.S. 1990. Mechanism of calcium transport across the plasma membrane of bovine chromaffin cells. *J. Neurochem.* **54**:1972–1979

Kersken, H., Vilmart-Seuwen, J., Momayezi, M., Plattner, H. 1986. Filamentous actin in *Paramecium* cells: Mapping by phalloidin affinity labeling in vivo and in vitro. *J. Histochem. Cytochem.* **34**:443–454

Khodorov, B.I. 1985. Batrachotoxin as a tool to study voltage-sensitive sodium channels of excitable membranes. *Prog. Biophys. Mol. Biol.* **45**:57–148

Knoll, G., Braun, C., Plattner, H. 1991. Quenched flow analysis of exocytosis in *Paramecium* cells: Time course, changes in membrane structure, and calcium requirements revealed after rapid mixing and rapid freezing of intact cells. *J. Cell Biol.* **113**:1295–1304

Knoll, G., Grässle, A., Braun, C., Probst, W., Höhne-Zell, B., Plattner, H. 1993. A calcium influx is neither strictly associated with nor necessary for exocytotic membrane fusion in *Paramecium* cells. *Cell Calcium* **14**:189–199

Knoll, G., Kerboeuf, D., Plattner, H. 1992. A rapid calcium influx during exocytosis in *Paramecium* cells is followed by a rise in cyclic GMP within 1 s. *FEBS Lett.* **304**:265–268

Kung, C., Saimi, Y., Martinac, B. 1990. Mechano-sensitive ion channels in microbes and the early evolutionary origin of solvent sensing. *Curr. Top. Membr. Transp.* **36**:145–153

Lumpert, C.J., Kersken, H., Plattner, H. 1990. Cell surface complexes ('cortices') isolated from *Paramecium tetraurelia* cells as a model system for analysing exocytosis in vitro in conjunction with microinjection studies. *Biochem. J.* **269**:639–645

Machemer, H. 1988. Electrophysiology. *In: Paramecium.* H.D. Görtz, editor. pp. 185–215. Springer-Verlag, Berlin, Heidelberg

Matt, H., Plattner, H. 1983. Decoupling of exocytotic membrane fusion from protein discharge in *Paramecium* cells. *Cell Biol. Int. Rep.* **7**:1025–1031

Mozhayeva, G.N., Naumov, A.P., Negulyaev, Y.A., Nosyreva, E.D. 1977. The permeability of aconitine-modified sodium channels to univalent cations in myelinated verve. *Biochim. Biophys. Acta* **466**:461–473

Ogura, A., Takahashi, K. 1976. Artificial deciliation causes loss of calcium-dependent responses in *Paramecium. Nature* **264**:170–172

Olbricht, K., Plattner, H., Matt, H. 1984. Synchronous exocytosis in *Paramecium* cells II. Intramembranous changes analysed by freeze-fracturing. *Exp. Cell Res.* **151**:14–20

Plattner, H. 1989. Regulation of membrane fusion during exocytosis. *Int. Rev. Cytol.* **119**:197–286

Plattner, H., Knoll, G., Pape, R. 1993. Synchronization of different steps of the secretory cycle in *Paramecium tetraurelia:* Trichocyst exocytosis, exocytosis-coupled exocytosis, and intracellular transport. *In:* Membrane Traffic in Protozoa. H. Plattner, editor. pp. 123–148. JAI Press, Greenwich, CT, London

Plattner, H., Lumpert, C.J., Knoll, G., Kissmehl, R., Höhne, B., Momayezi, M., Glas-Albrecht, R. 1991. Stimulus-secretion coupling in *Paramecium* cells. *Eur. J. Cell Biol.* **55**:3–16

Plattner, H., Matt, H., Kersken, H., Haacke, B., Stürzl, R. 1984. Synchronous exocytosis in *Paramecium* cells. A novel approach. *Exp. Cell Res.* **151**:6–13

Plattner, H., Reichel, K., Matt, H., Beisson, J., Lefort-Tran, M., Pouphile, M. 1980. Genetic dissection of the final exocytosis steps in *Paramecium tetraurelia* cells: Cytochemical determination of Ca^{2+}-ATPase activity over preformed exocytosis sites. *J. Cell Sci.* **46**:17–40

Plattner, H., Stürzl, R., Matt, H. 1985. Synchronous exocytosis in *Paramecium* cells IV. Polyamino compounds as potent trigger agents for repeatable trigger-redocking cycles. *Eur. J. Cell Biol.* **36**:32–37

Preston, R.R. 1990. Genetic dissection of Ca^{2+}-dependent ion channel function in *Paramecium. BioEssays* **12**:273–281

Preston, R.R., Saimi, Y. 1990. Calcium ions and the regulation of motility in *Paramecium. In:* Ciliary and Flagellar Membranes. R.A. Bloodgood, editor, pp. 173–200. Plenum, New York, London

Preston, R.R., Saimi, Y., Kung, C. 1992. Calcium current activated upon hyperpolarization of *Paramecium tetraurelia. J. Gen. Physiol.* **100**:233–251

Saimi, Y. 1986. Calcium-dependent sodium currents in *Paramecium:* Mutational manipulations and effects of hyper- and depolarization. *J. Membrane Biol.* **92**:227–236

Saimi, Y., Kung, C. 1980. A Ca-induced Na-current in *Paramecium. J. Exp. Biol.* **88**:305–325

Satow, Y., Kung, C. 1980. Membrane currents of pawn mutants of the pwA group in *Paramecium tetraurelia. J. Exp. Biol.* **84**:57–71

Schultz, J.E., Pohl, T., Klumpp, S. 1986. Voltage-gated Ca^{2+} entry into *Paramecium* linked to intraciliary increase of cyclic GMP. *Nature* **322**:271–273

Schultz, J.E., Schade, U. 1989. Veratridine induces a Ca^{2+} influx, cyclic GMP formation, and backward swimming in *Paramecium tetraurelia* wild-type cells and Ca^{2+} current-deficient pawn mutant cells. *J. Membrane Biol.* **109**:251–258

Stelly, N., Mauger, J.P., Kéryer, G., Claret, M., Adoutte, A. 1991. Cortical alveoli of *Paramecium.* A vast submembranous calcium compartment. *J. Cell Biol.* **113**:103–112

Uezono, Y., Wada, A., Yanagihara, N., Kobayashi, H., Mizuki, T., Terao, T., Koda, Y., Izumi, F. 1992. Veratridine causes the Ca^{2+}-dependent increase in diacylglycerol formation and translocation of protein kinase C to membranes in cultured bovine adrenal medullary cells. *Arch. Pharmacol.* **346**:76–81